



HAL
open science

Restoring robust binary switching operation and exceptional point using long-period grating-assisted parity-time symmetric couplers

Vincent Brac de La Perrière, Quentin Gaimard, Henri Benisty, Abderrahim Ramdane, Anatole Lupu

► **To cite this version:**

Vincent Brac de La Perrière, Quentin Gaimard, Henri Benisty, Abderrahim Ramdane, Anatole Lupu. Restoring robust binary switching operation and exceptional point using long-period grating-assisted parity-time symmetric couplers. *Journal of Physics D: Applied Physics*, 2019, 52 (25), pp.255103. 10.1088/1361-6463/ab11b4 . hal-02336274

HAL Id: hal-02336274

<https://hal.science/hal-02336274>

Submitted on 28 Oct 2019

HAL is a multi-disciplinary open access archive for the deposit and dissemination of scientific research documents, whether they are published or not. The documents may come from teaching and research institutions in France or abroad, or from public or private research centers.

L'archive ouverte pluridisciplinaire **HAL**, est destinée au dépôt et à la diffusion de documents scientifiques de niveau recherche, publiés ou non, émanant des établissements d'enseignement et de recherche français ou étrangers, des laboratoires publics ou privés.

Restoring robust binary switching operation and exceptional point using long-period grating-assisted Parity-Time symmetric couplers

Vincent Brac de la Perrière¹, Quentin Gaimard¹, Henri Benisty², Abderrahim Ramdane¹, and Anatole Lupu¹

¹Centre de Nanosciences et de Nanotechnologies, CNRS, Univ. Paris-Sud, Université Paris-Saclay, C2N – 10 Boulevard Thomas Gobert – 91120 Palaiseau cedex, France

²Laboratoire Charles Fabry de l'Institut d'Optique, CNRS, Univ. Paris Saclay, 2 Ave Augustin Fresnel, 91127 Palaiseau Cedex, France

E-mail: anatole.lupu@c2n.upsaclay.fr

Received xxxxxx
Accepted for publication xxxxxx
Published xxxxxx

Abstract

The impact of imbalance in waveguides propagation constants among Parity-Time symmetric coupled waveguides and/or of a complex-valued coupling coefficient is assessed. The narrow tolerance found implies that attempts to tightly control waveguides parameters appear as elusive because of fabrication technology limitations, calling for more feasible mitigation avenues. It is shown that a grating-assisted Parity-Time symmetric coupler design restores both technologically robust binary switching operation and exceptional point. In addition the proposed design is compatible with birefringence compensation techniques providing polarization-independent operation as well as coupling and/or gain-loss profile modulation techniques that extend the control of switching operation in the Parity-Time symmetric phase. Using wavelength as an additional tuning parameter near exceptional points opens promising avenues for manipulating the trajectory on Riemann sheets in topological photonics applications.

Keywords: Parity-Time symmetry, Integrated optics, Optical switching

1. Introduction

The proposal in 1998 by Bender and Boettcher of the concept of “non-Hermitian Hamiltonians” obeying parity-time (PT) symmetry as a complex extension of conventional quantum mechanics quickly became a new paradigm in theoretical physics [1,2]. The distinctive feature of this special class of antilinear symmetry non-Hermitian Hamiltonians [3] is that under certain conditions they can have a completely real spectrum. This property is referred as exact PT-symmetry. In the opposite case the PT symmetry is

said to be broken. At the transition point between exact and broken PT-symmetry two or more of the real eigenvalues of the Hamiltonian coalesce [4,5], leading to an “exceptional point” (EP) [6].

Aside the pure intellectual interest of this topic, it became clear that PT-symmetry is also of utmost relevance in photonics. Because of the formal equivalence between such operators and coupled-modes equations, optics provides growing opportunities for the implementation and experimental investigation of PT-symmetry-type systems (PTSS) [7-11]. A pair of coupled waveguides with gain and loss sketched in figure 1(a) represents the simplest

configuration of PT-symmetric optical system (PTSS), which was extensively studied in view of optical signals manipulation [8,12-23] or of terahertz devices [24,25].

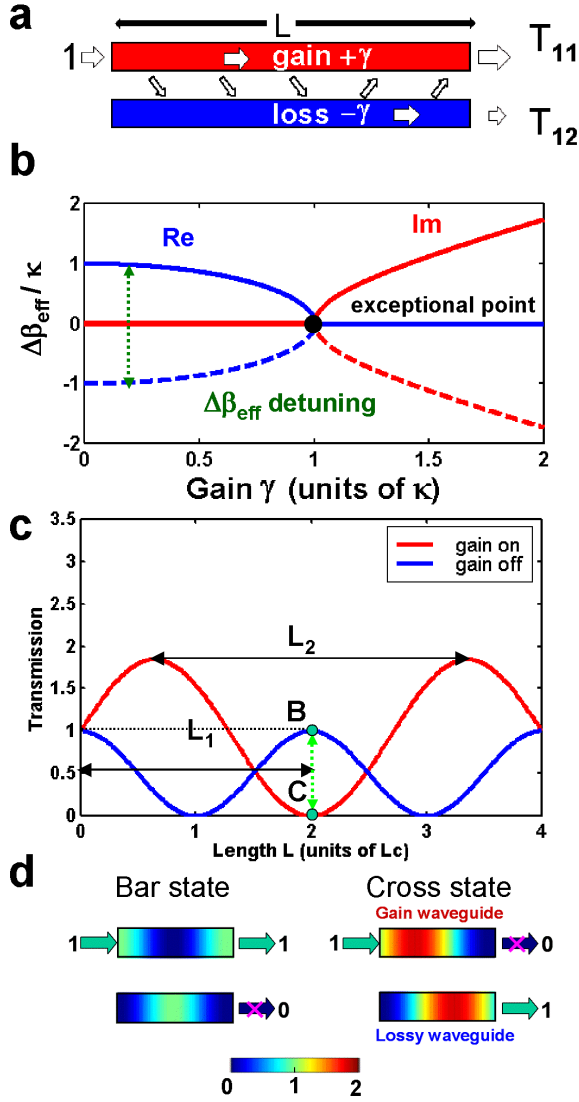


Figure 1. a) Sketch of a PT-symmetric directional coupler; b) Operation at zero detuning ($\delta=0$). Real parts (“Re”, blue lines) and Imaginary parts (“Im”, red lines) of the complex eigenvalues difference $\Delta\beta$, normalized to the coupling coefficient κ ; c) Intensity distribution along the gain waveguide for a PTSS with gain-loss level $\gamma=0$ (blue line) and $\gamma=0.6765\kappa$ (red line); At point B, power in the other guide (not shown) vanishes exactly if $\delta=0$, whereas at point C, the exact zero output is in the input guide. d) Color-coded switching operation for a PTSS with gain-loss level $\gamma=0$ (bar state - left) and $\gamma=0.6765\kappa$ (cross state - right), the colormap can be read from the correspondence of the top guide of the two cases to the two plots of (c).

In such a PTSS the effective detuning of the propagation constants between the odd and even supermodes (i.e., propagation eigenvalues difference $\Delta\beta=\beta_o-\beta_e$ between odd and even supermodes) is gradually reduced upon increasing the level of combined gain/loss in the system until the imaginary parts of these constants merge at the exceptional point [figure 1(b)]. The variation of $\Delta\beta$ [figure 1(c)], which is inversely proportional to $\Delta\beta$ [figure 1(c)], can be advantageously exploited for implementing switches and modulators [figure 1(d)].

Several such studies focused their attention on the singular properties of PTSS related to the abrupt evolution of propagation constants $\beta'+i\beta''$ in the vicinity of the EP [14,16-20] and manipulation of the trajectory on Riemann sheets in a growing number of topological photonics applications [24,25]. Experimentally however, achieving operation right at the EP is far from being trivial. The main factors causing the smearing of EP are the imbalance in propagation constants of coupled waveguides [19,20] and/or a complex-valued coupling coefficient [18,19]. To circumvent these issues, the solution proposed in [19] to recover the the EP is to consider a design with vertically stacked waveguides having different core thickness. The phase matching condition between non-identical waveguides is obtained by using for the core a dispersive material of very high gain ($\sim 1500\text{ cm}^{-1}$).

The aim of this Letter is to propose a more affordable solution in terms of gain (loss) level. For 1-mm length-scale device, the required gain (loss) level of our design does not exceed $\sim 45\text{ cm}^{-1}$ (i.e. 200 dB/cm). Furthermore, this design not only ensures a robust recovery of the EP, but it is also perfectly suited for binary switching operation below EP as presented in [26,27]. In addition it does not impair the use of birefringence compensation technique for achieving polarization-independent operation [28].

2. Imbalance in modal index on EP and switching

To present our approach, we start with the simplest model of two coupled waveguides, one with gain and the other with balanced losses. We consider two scalar fields q_1 and q_2 propagating in these waveguides and described by the system:

$$\frac{dq_1}{dz} = (\beta_1 + i\gamma)q_1 + \kappa q_2, \quad \frac{dq_2}{dz} = \kappa q_1 + (\beta_2 - i\gamma)q_2 \quad (1)$$

where $\kappa=\kappa'+i\kappa''$ is the complex-valued coupling coefficient while γ is the z-invariant gain-loss coefficient. The eigenvalues of propagation constants in the system are:

$$\sigma = \frac{\beta_1 + \beta_2}{2} \pm \sqrt{\kappa'^2 + \delta^2 - \gamma^2 + 2i(\delta\gamma + \kappa'\kappa'')} \quad (2)$$

Here the convenient variable $\delta = (\beta_1 - \beta_2)/2$ is the half-detuning of the waveguides propagation constants. As evident from Eq. (2) the presence of an imaginary term in the square-root of Eq. (2) leads to complex eigenvalues, and

further results in the smearing of the EP. The ratio $|\delta+\kappa|/\kappa$ may serve as a measure of deviation from the ideal case i.e., the EP. To evaluate the impact of the detuning δ , the deviation of waveguides propagation constants, whose limits are dictated by technological imperfections, we assume for the moment that $\kappa'' = 0$. Expressing a meaningful condition of a “small” detuning around EP then involves the coupling length $L_c = \pi/2\kappa$ as follows:

$$\frac{\delta}{\kappa} = \frac{L_c}{\lambda} (n_1 - n_2) \ll 1 \quad (3)$$

where n_j is the waveguide j modal (effective) index. For 1-mm scale coupling length typical for integrated optics and 1- μm scale wavelength, the detuning is negligible when the effective index difference $\Delta n = (n_1 - n_2)$ obeys $\Delta n \ll 10^{-3}$. The detrimental impact of the waveguides effective index difference Δn on the EP is illustrated in figure 2(a). As can be seen, when $\Delta n = 10^{-3}$, the evolution of coupled waveguides eigenvalues as a function of γ widely differs from evolution in the ideal case $\Delta n = 0$. For $\Delta n = 10^{-4}$ some resemblance of eigenvalues curves with respect to the ideal case is retrieved, though large deviations subsist even far from the EP. When $\Delta n = 10^{-5}$ a global behavior approaching to that of an ideal case is recovered, except in the near vicinity of EP [see inset in figure 2(a)]. One important parameter that motivated the quest for operating at the EP is the steep variation of eigenvalues ($d\sigma/d\gamma$) in its near vicinity. In the presence of finite detuning δ the maxima for real and imaginary components of $d\sigma/d\gamma$ are achieved at the inflection points of corresponding branches, i.e. $\text{Re}(\sigma)$ and $\text{Im}(\sigma)$. In contrast to the ideal case $\delta = 0$, the maxima of $d[\text{Re}(\sigma)]/d\gamma$ and $d[\text{Im}(\sigma)]/d\gamma$ on the abscissa axis γ split and go below and above the EP, respectively. Furthermore, as shown in the Appendix A, the maxima are equidistant (albeit to first order only) from the exact EP ($\gamma/\kappa = 1$):

$$\frac{\gamma_{\text{Re}}}{\kappa} = \sqrt{1 + \frac{4\delta^2}{3\kappa^2} - \frac{1}{\sqrt{3}} \frac{|\delta|}{\kappa}}, \quad \frac{\gamma_{\text{Im}}}{\kappa} = \sqrt{1 + \frac{4\delta^2}{3\kappa^2} + \frac{1}{\sqrt{3}} \frac{|\delta|}{\kappa}} \quad (4)$$

Note, that despite this is a linear approximation when $\delta/\kappa \ll 1$, the derivatives $d\text{Re}(\sigma)/d\gamma$ and $d\text{Im}(\sigma)/d\gamma$ are tending toward the same limit:

$$\lim_{\delta \rightarrow 0} \frac{\partial \text{Re}(\sigma)}{\partial \gamma} = \lim_{\delta \rightarrow 0} \frac{\partial \text{Im}(\sigma)}{\partial \gamma} \approx \sqrt[4]{\frac{27}{16}} \sqrt{\frac{\kappa}{|\delta|}} \quad (5)$$

As follows from Eq. (5) the steepness of eigenvalues derivatives $d\sigma/d\gamma$ in the near vicinity of EP grows only as $\delta^{-1/2}$. It means that in order to increase by an order of magnitude $d\sigma/d\gamma$ from the modest value of 10^1 observed for $\Delta n = 10^{-5}$ up to a more palatable 10^2 target, the index detuning should be reduced by two orders of magnitude, down to $\Delta n = 10^{-7}$, which is all but attainable with any foreseeable technologies.

To illustrate this we consider a typical design of III-V semiconductor waveguide with butyl-cyclo-benzene (BCB)

overclad represented as inset in figure 3. The numerically calculated dependence of TE polarization effective index as a function of waveguide width w is displayed in figure 3. As can be seen for $w \sim 2 \mu\text{m}$, corresponding to the single mode operation, a variation of waveguide width by 100 nm leads to a change in effective index $\Delta n = 10^{-3}$. Thus, to achieve $\Delta n = 10^{-5}$, the width of the two coupler waveguides should be identical within an accuracy of 1 nm. And to achieve a detuning of $\Delta n = 10^{-7}$, a sub-atomic precision level is required. Consequently, the capability to control detuning through waveguides geometry and material parameters is definitely quite elusive.

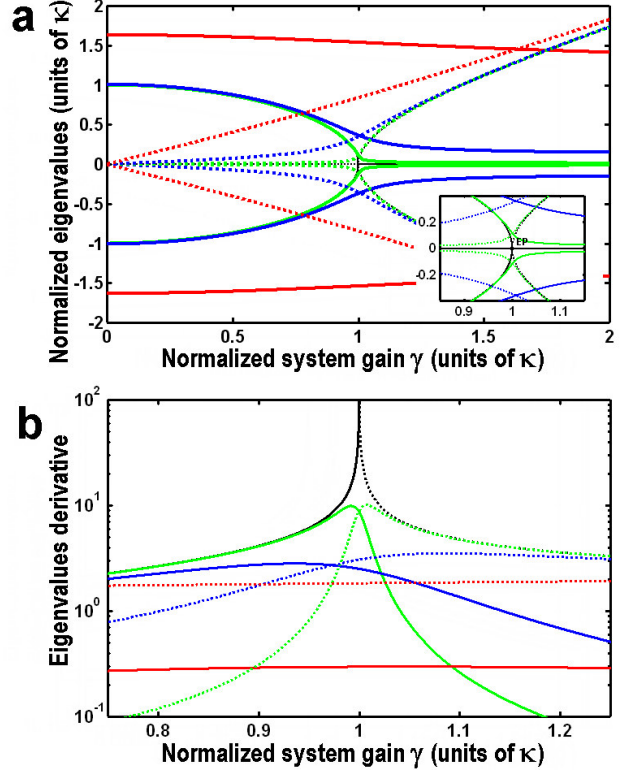


Figure 2. Evolution of eigenvalues in a system of PT-symmetric waveguides with different values of detuning (black: $\Delta n = 0$, green: $\Delta n = 10^{-5}$, blue: $\Delta n = 10^{-4}$, red: $\Delta n = 10^{-3}$). a) Real parts (solid lines) and Imaginary parts (dotted lines) of the two normalized and offset eigenvalues, i.e. $\sigma - (\beta_1 + \beta_2)/2$, with a zoom of the EP in the inset; b) Derivatives of the Real parts (solid lines) and Imaginary parts (dotted lines) of the eigenvalues $d\sigma/d\gamma$.

Similar findings, which are detailed in Appendix B, hold when considering switching operation in the PT-symmetric phase below EP [26]. Traditionally, such “2x2” four-port devices operate either in the so-called *bar* state sketched in left panel figure 1(d) or in the *cross* state [29] [right panel in figure 1(d)]. To tackle the switch we consider the evolution of the input “binary” state $(e^{-i\phi}, 0)^T$, [hereafter T stands for

the transpose]. We want the output of the device $z = L$ to be either bar state ($T_{11}=1, T_{12}=0$) or cross state ($T_{11}=0, T_{12}=1$). For the considered coupler of length $L = 2.1 L_c$ with constant coupling and gain-loss profile, the lowest binary state is *bar*. It is achieved when $\gamma \approx 0.3 \kappa$. The second binary state corresponding to the switching operation from *bar* to *cross* is achieved at $\gamma \approx 0.7 \kappa$. The detrimental effect of effective index detuning appears in figure 4. Almost perfect switching operation with very low level of zero (< -40 dB) is observed when $\Delta n = 10^{-6}$ [see figure 4(a)]. When $\Delta n = 10^{-5}$ the switching is still acceptable with the level zero ~ -20 dB [see figure 4(b)]. But further increase of detuning up to $\Delta n = 10^{-4}$ totally compromises the switching operation [see figure 4(c)].

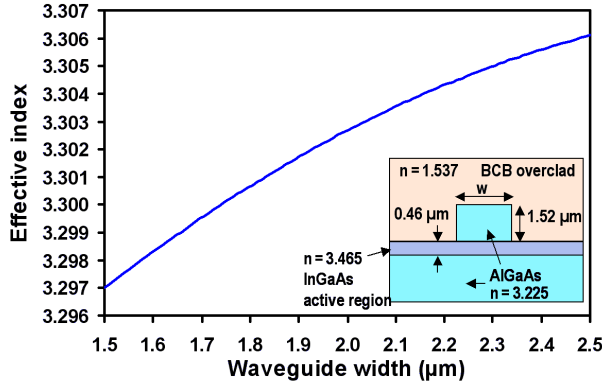


Figure 3. Effective index dispersion as function of waveguide width w . Inset: Sketch of an AlGaAs/InGaAs rib waveguide with BCB overclad (values of refractive indices are indicated for $\lambda = 1.55 \mu\text{m}$).

We make the point here that the situation of switching is particularly sensitive because it is the quest of a perfect zero of the scattering matrix. Thus we are going to show that it is nearly as sensitive for the switching as it is around the EP. In the case of switching, we show in Appendix B that we have a linear dependence of the departures from zero, in the form of the imaginary part of $\cos(\Omega L)$ and $\sin(\Omega L)$ that define $q_1(L)$. In the case of the EP, we show that the derivatives of the eigenvalues, instead of being steep, are stalling at points for which we establish an analytical formulation in Appendix A, which turns out to have a quite similar behaviour.

Similar behavior for the switching operation and EP is observed when the impact of complex valued coupling coefficient $\kappa = \kappa' + i\kappa''$ instead of detuning is considered. The measure of smallness in this case is given by the κ''/κ' ratio.

It should be noted that as follows from Eq. (2) the negative impact of κ'' can be compensated by a judicious introduction of detuning δ and vice versa. The associated analysis was performed in refs [18] and [19]. The issue is that for a fixed detuning δ the impact of κ'' can be corrected

only for a single gain point on the eigenvalues dispersion diagram $\sigma(\gamma)$, when meeting the condition:

$$\delta\gamma + \kappa'\kappa'' = 0 \quad (6)$$

The alternative solution, proposed in [19] consists in compensating detuning by using complex valued coupling coefficient. This provides some freedom to tune the operation point on the $\sigma(\gamma)$ diagram, but, as said, requires huge gain levels. Hence, this solution is not satisfactory either.

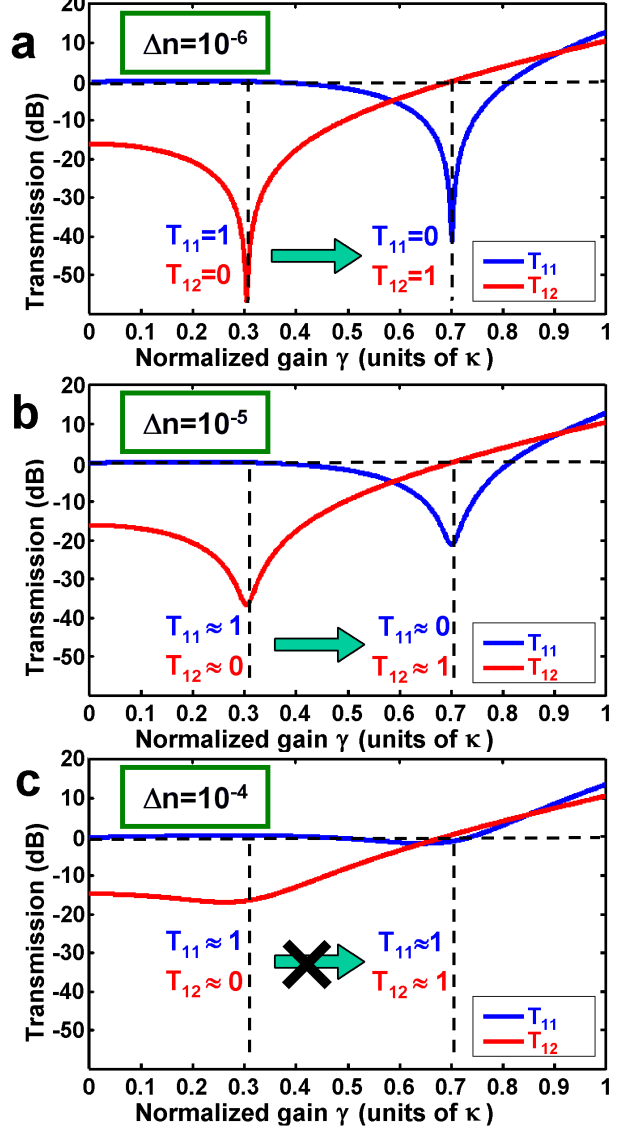


Figure 4. Switching operation of conventional PT-symmetric coupler of length $L = 2.1 L_c$ (slightly longer than in Fig.1, hence the bar and cross points are shifted to $\gamma \approx 0.3 \kappa$ and $\gamma \approx 0.7 \kappa$) for different values of detuning. a) $\Delta n = 10^{-6}$; b) $\Delta n = 10^{-5}$; c) $\Delta n = 10^{-4}$.

3. Restoring EP and binary switching using long-period grating-assisted PT-symmetric couplers

As follows from Eq. (6) the situation can be remediated if it is possible to modulate the detuning as function of some parameter. The wavelength becomes such a parameter in two interesting cases. Firstly, an asymmetric directional coupler design [30] naturally makes dispersion curves coincide at some wavelength λ_0 ensuring thus the phase matching condition $\beta_1(\lambda_0) = \beta_2(\lambda_0)$. In a linear expansion $\beta_j(\lambda) = \beta_j(\lambda_0) + (\lambda - \lambda_0) d\beta_j/d\lambda$ the detuning δ can be expressed as:

$$\delta = (\lambda - \lambda_0) d(\beta_1 - \beta_2)/d\lambda \quad (7)$$

The typical value of the index dispersion, $d(n_1 - n_2)/d\lambda$, for III-V semiconductor waveguides is $\sim 0.01 \mu\text{m}^{-1}$, meaning that the required control on the wavelength positioning to attain a detuning $\Delta n < 10^{-7}$ is then of the order of 10^{-2} nm , which is quite common with existing tunable semiconductor laser sources.

The second case, more convenient to hit an adapted detuning (say $\Delta n \sim 10^{-6}$) is to use long period grating assisted directional couplers [GADC, see figure 5(a)] providing greater degree of freedom for the choice of materials and design of the waveguides. The phase matching condition in this case reads:

$$\beta_1(\lambda_0) - \beta_2(\lambda_0) = 2\pi/\Lambda \Leftrightarrow \lambda_0 = \Lambda \cdot [n_1(\lambda_0) - n_2(\lambda_0)] \quad (8)$$

where Λ is the grating period, typically on the order of few tens of microns. Furthermore, the birefringence compensation technique originally proposed in [28] and experimentally demonstrated in [31,32] allows achieving polarization-independent operation.

To this end a condition of identical TE and TM birefringence should be met through appropriate guide design (material composition and geometry):

$$n_1^{\text{TE}} - n_1^{\text{TM}} = n_2^{\text{TE}} - n_2^{\text{TM}} \quad (9)$$

To examine the switching behaviour of grating assisted PT-symmetric coupler we consider the example of device with length $L = 2.0L_c = 2 \text{ mm}$, $n_1 = 3.3$, $n_2 = 3.25$, $\Lambda = 30 \mu\text{m}$. According to Eq. (7) the phase matching condition is met at $\lambda_0 = 1.5 \mu\text{m}$. For the given coupler length the *bar* state occurs for $\gamma = 0$ and the *cross* state is achieved when $\gamma \approx 0.677\kappa$ corresponding to amplification level γL of 18.5 dB [26]. The impact of introducing additional detuning Δn between waveguides is illustrated in figures 5(b-d). To perform this modeling we used the conventional coupled mode theory formalism of transfer matrix [33].

As can be observed, perfect switching operation is now successfully observed even for $\Delta n = 10^{-3}$, though at the expense of a $\sim 30 \text{ nm}$ shift of the phase-matching wavelength, see figure 5(d). The phase matching wavelength is red-

shifted if $\Delta n > 0$ and blue-shifted if $\Delta n < 0$. The shift scales linearly with Δn and is thus down to $\Delta\lambda_0 \approx 1 \text{ nm}$ for a feasible target $\Delta n \approx 3.3 \cdot 10^{-5}$. Such shifts from the nominal value can be commonly compensated using for instance a thermal tuning mechanism [32].

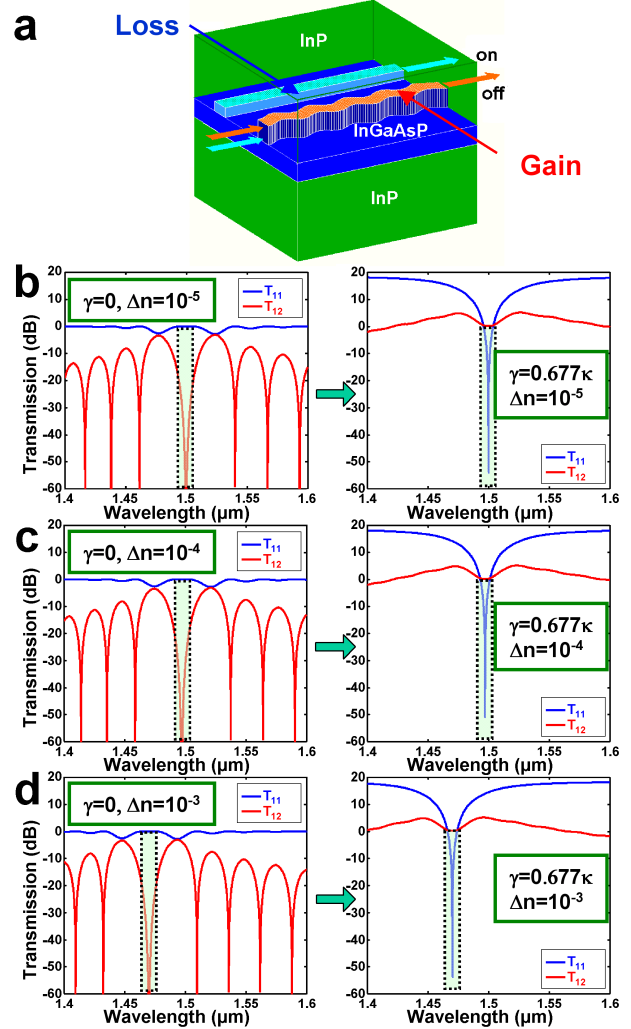


Figure 5. Switching operation of grating assisted PT-symmetric coupler of length $L = 2 L_c$ for different values of detuning, whereby perfect switching is achieved albeit at the expense of a shifted wavelength. a) $\Delta n = 10^{-5}$; b) $\Delta n = 10^{-4}$; c) $\Delta n = 10^{-3}$.

For InGaAsP with a quaternary alloy composition corresponding to $\lambda_g \approx 1.5 \mu\text{m}$ bandgap wavelength, according the expressions and values given in [34], an index variation $\Delta n/\Delta T = 4 \times 10^{-4}$ is theoretically expected. A temperature variation of 25°C could thus be sufficient to obtain a variation of index of 10^{-2} . Based on this approach an electrical wavelength tuning control was experimentally demonstrated in [32]. To this end a 400nm thick Ti film was

evaporated and stripped by a lift-off technique to form a thin-film heater of 40 μm strip width overlaying both GADC waveguides. A greater than 20nm tuning range with a remarkable polarisation isotropy was achieved. The electrical power consumption around 0.3W could be further reduced at least by a factor of two by optimizing the design of heating electrodes.

Note also that the amplification (attenuation) γL required for switching can be reduced down to only 13.6 dB level by considering an appropriate square longitudinal modulation of the gain-loss profile as detailed in a recent optimization study [27].

We can now come back to the issue of encircling the EP, which entails a circulation on different Riemann sheets. The solution proposed by the GACD mitigates the structural detuning by a wavelength detuning. We can therefore conclude that by scanning the injected light wavelength and gain/loss level in an adequate way we will encircle the EP for a plausibly reasonable span of wavelengths.

4. Summary and conclusion

In summary, the impact of effective index detuning in a system of PT-symmetric coupled waveguides is considered. It is shown that for a 2-mm-long coupler, the achievement of EP as well as switching operation in PT-symmetric phase requires a detuning typically lower than $\Delta n \sim 10^{-5}$. Achieving a detuning below this limit seems elusive because of tight constraints imposed on fabrication technology. To circumvent these issues a long-period grating-assisted PT-symmetric coupler design was considered and shown to perform well at the expense of a manageable wavelength shift. The proposed solution advantageously restores robust binary switching operation and exceptional point. In addition such design is compatible with birefringence compensation techniques providing polarization-independent operation as well as with gain-loss or coupling longitudinal profile tailoring allowing reduction of amplification (attenuation) level with respect to the conventional uniform PT-symmetric coupler design. The introduction in PT-symmetric systems of the wavelength as an additional tuning parameter around the exceptional point opens promising avenues for manipulating the trajectory on Riemann sheets in topological photonics applications.

Acknowledgements

This work was supported by the French Agence Nationale pour la Recherche (project "PARTISYMO", contract number N° ANR-18-CE24-0024-01).

Appendix A. Determination of $d\sigma/d\gamma$ extrema

To calculate the impact of modal index imbalance δ on the eigenvalue sensitivity to gain $d\sigma/d\gamma$ in the vicinity of EP, let us consider for the sake of simplicity that $\kappa'' = 0$. Then, as follows directly from Eq. (2):

$$\frac{\partial \sigma}{\partial \gamma} = \frac{-\gamma + i\delta}{\sqrt{\kappa^2 + \delta^2 - \gamma^2 + 2i\delta\gamma}} \quad (\text{A.1})$$

To find the loci of extrema for real and imaginary parts of $d\sigma/d\gamma$ let us introduce for convenience $V = \sqrt{\kappa^2 + \delta^2 - \gamma^2 + 2i\delta\gamma}$ (A.2)

Since $dV/d\gamma = -(\gamma - i\delta)/V$ it then follows that:

$$\frac{\partial^2 \sigma}{\partial^2 \gamma} = \frac{\kappa^2}{V^3} \quad (\text{A.3})$$

By introducing the auxiliary variables:

$$a = \sqrt{\kappa^2 + \delta^2 - \gamma^2} \text{ and } b = \sqrt{2\delta\gamma} \quad (\text{A.4})$$

we get:

$$\frac{\partial^2 \sigma}{\partial^2 \gamma} = \kappa^2 \frac{(\sqrt{a - ib})^3}{(a^2 + b^2)^3} \quad (\text{A.5})$$

Note now:

$$c = \rho e^{-i\varphi} = a - ib \quad (\text{A.6})$$

where $\rho = \sqrt{a^2 + b^2}$ and $\tan(\varphi) = \frac{b}{a}$ (A.7)

Then $\sqrt{c^3} = \sqrt{\rho^3} [\cos(3\varphi/2) - i \sin(3\varphi/2)]$ (A.8)

The condition for $\text{Re}[d^2\sigma/d^2\gamma] = 0$ implies that $\varphi = \pi/3$. By using Eq. (A.7) we obtain:

$$a = \frac{b}{\sqrt{3}} \Leftrightarrow \kappa^2 - \gamma^2 + \delta^2 = \frac{2}{\sqrt{3}} \delta\gamma \quad (\text{A.9})$$

The Eq. (A.9) is satisfied when:

$$\gamma_{\text{re}} = -\frac{\delta}{\sqrt{3}} \pm \sqrt{\kappa^2 + 4\frac{\delta^3}{3}} \quad (\text{A.10})$$

In a similar manner, the extremum for the imaginary part of $d\sigma/d\gamma$ is achieved when $\varphi = 2\pi/3$. It corresponds to the condition:

$$a = -\frac{b}{\sqrt{3}} \Leftrightarrow \kappa^2 - \gamma^2 + \delta^2 = -\frac{2}{\sqrt{3}} \delta\gamma \quad (\text{A.11})$$

This is satisfied when:

$$\gamma_{\text{im}} = \frac{\delta}{\sqrt{3}} \pm \sqrt{\kappa^2 + 4\frac{\delta^3}{3}} \quad (\text{A.12})$$

Appendix B. Impact of modal index imbalance on PT-symmetric coupler switching operation

As illustrated in figure 3 in a binary switching operation the modal index imbalance primarily affects the extinction level (the missed zero). For a PT-symmetric coupler of length L with uniform gain-loss and coupling profiles the transmission in *bar* state is [23]:

$$q_1 = \cos(\Omega L) + \frac{\gamma + i\delta}{\Omega} \sin(\Omega L) \quad (\text{B.1})$$

where

$$\Omega = \sqrt{\kappa^2 + \delta^2 - \gamma^2 + 2i\delta\gamma} \quad (\text{B.2})$$

Considering a linear approximation when the detuning δ is small we get:

$$\Omega \approx \Omega_0 + i \frac{\delta\gamma}{\Omega_0} = \Omega_0 + i\Omega'' \quad (\text{B.3})$$

where:

$$\Omega_0 = \sqrt{\kappa^2 - \gamma^2}; \quad \Omega'' = \frac{\delta\gamma}{\Omega_0} \quad (\text{B.4})$$

As detailed in [23], the following relations holds when $q_1=0$:

$$\sin(\Omega_0 L) = \frac{\Omega_0}{\kappa}; \quad \cos(\Omega_0 L) = -\frac{\gamma}{\kappa} \quad (\text{B.5})$$

Using Eqs. (B.3) and (B.5) as well as the smallness of the detuning $\delta \ll \Omega_0$, we obtain the new values for the detuned case with a linear-in- δ expansion (through Ω'') as:

$$\sin(\Omega L) = \frac{\Omega_0}{\kappa} - i \frac{\gamma}{\kappa} \Omega'' L; \quad \cos(\Omega_0 L) = -\frac{\gamma}{\kappa} - i \frac{\Omega_0}{\kappa} \Omega'' L \quad (\text{B.6})$$

As follows from Eq. (B.1), the presence of additional terms in Eqs. (B.6) caused by the modal index imbalance breaks the condition $q_1=0$ required for binary switching operation.

References

- [1] Bender CM and Boettcher S 1998 *Phys. Rev. Lett.* **80** 5243.
- [2] Bender CM and Boettcher S 2007 *Rep. Prog. Phys.* **70** 947–1018
- [3] Mostafazadeh A 2002 *J. Math. Phys.* **43** 205
- [4] Bender CM, Berry MV, and Mandilara A 2002 *J. Phys. A* **35** L467
- [5] Dorey P, Dunning C, Tateo R 2001 *J. Phys. A* **34**, L391
- [6] Kato T 1966 *Perturbation Theory of Linear Operators* (Berlin: Springer)
- [7] Guo A, Salamo GJ, Duchesne D, Morandotti R, Volatier-Ravat M, Aimez, Siviloglou GA, and Christodoulides DN 2009 *Phys. Rev. Lett.* **103** 093902
- [8] Rüter CE, Makris KG, El-Ganainy R, Christodoulides DN, Segev M, and Kip D 2010 *Nature Phys.* **6**, 192–195
- [9] Kottos T 2010 *Nature Phys.* **63** 166–167
- [10] Feng L, Xu YL, Fegadolli WS, Lu MH, Oliveira JE, Almeida VR, Chen YF, and Scherer A 2012 *Nat. Mater.* **12** 108–113
- [11] Peng B, Özdemir ŞK, Lei F, Monifi F, Gianfreda M, Long GL, Fan S, Nori F, Bender CM, Yang L 2014 *Nature Physics* **10**, 394–398
- [12] Chu PL, Peng GD, Malomed BA, Hatami-Hanza H, and Skinner I 1995 *Opt. Lett.* **20**, 1092-1094
- [13] Malomed BA, Peng GD, and Chu PL 1996 *Opt. Lett.* **21**, 330–332
- [14] Klaiman S, Günther U, and Moiseyev N 2008 *Phys. Rev. Lett.* **101** 080402
- [15] Čtyroký J, Kuzmiak V, and Eyderman S 2010 *Opt. Express* **18**, 21585–21593
- [16] Benisty H, Degiron A, Lupu A, De Lustrac A, Chénais S, Forget S, Besbes M, Barbillon G, Bruyant A, Blaize S, and Lérondel G, 2011 *Opt. Express* **19** 18004-18019
- [17] Konotop VV, Shchesnovich VS, Zezyulin DA 2012 *Phys. Lett. A* **376** 2750-2753
- [18] Benisty H, Yan C, Degiron A, and Lupu AT 2012 *J. Lightwave Technol.* **30** 2675–2683
- [19] Nguyen NB, Maier AA, Hong M, and Oulton RF 2016 *New J. Phys.* **18** 125012
- [20] Mortensen NA, Gonçalves PAD, Khajavikhan M, Christodoulides DN, Tserkezis C, and Wolff C 2018 *Optica* **5** 1342-1346
- [21] Gear J, Sun Y, Xiao S, Zhang L, Fitzgerald R, Rotter S, Chen H, and Li J 2017 *New J. Phys.* **19** 123041
- [22] Xiao S, Gear J, Rotter S, and Li J 2016 *New J. Phys.* **18** 085004.
- [23] Choi Y, Hahn C, Yoon JW, Song SH, and Berini P 2017 *Nat. Communications* **8** 14154
- [24] Zhang XL, Wang XB, and Chan CT 2018 *Phys. Rev. Appl.* **10** 034045
- [25] Ding K, Ma G, Zhang ZQ, and Chan CT 2018 *Phys. Rev. Lett.* **121** 085702
- [26] Lupu A, Benisty H, and Degiron A 2013 *Opt. Express* **21** 21651-21668
- [27] Lupu A, Konotop VV, and Benisty H 2016 *Scientific reports* **7** 13299
- [28] François S, Fouchet S, Bouadma N, Ougazzaden A, Carré M, Hervé-Gruyer G, Filoche M, Carenco A 1995 *IEEE Photonics Technol. Lett.* **7** 780-781
- [29] Kogelnik H, and Schmidt 1979 *IEEE J. Quantum Electron.* **12** 396
- [30] Wu C, Roland CC, Puetz N, Bruce R, Chick KD, Xu JM 1991 *IEEE Photonics Tech. Lett.* **3** 519-521
- [31] Lupu A, Sik H, Mereuta M, Boulet P, Carré M, Slemptes S, Ougazzaden A and Carenco A 2000 *Electronics Lett.* **36** 2030-2031
- [32] Lupu A, Win P, Sik H, Boulet P, Carre M, Landreau J, Slemptes S, Carenco A 1999 *Electronics Lett.* **35** 174-175
- [33] Huang WP, Lit JW 1991 *Journal of Lightwave Technology* **9** 845-852
- [34] Weber J P 1994 *IEEE J. Quantum Electron.* **30** 1801-1816